DESDE 2013
https://repository.uaeh.edu.mx/revistas/index.php/icbi/issue/archive
Pädi Boletín Científico de Ciencias Básicas e Ingenierías del ICBI
ISSN: 2007-6363

Publicación Semestral Pädi Vol. 14 No. 27 (2026) 1-8

Boosting solar energy: Recycled aluminum for the manufacture of diffuse reflectors
Potenciando la energía solar: Aluminio reciclado para la fabricación de reflectores difusos

G. V. Rodríguez-Martínez [a], M. Á. Ortega-González [a], F. Legorreta-García [a], D. Fuentes-Hernández* [a], L. E. Trujillo-Villanueva [a], V. Ramírez-Trejo [a], E. A. Chávez-Urbiola [b]

[a] *Laboratorio de Tecnología de Cerámicos (LTC), Área Académica de Ciencias de la Tierra y Materiales (AACTyM), Instituto de Ciencias Básicas e Ingeniería (ICBI), Universidad Autónoma del Estado de Hidalgo (UAEH) 42184, Pachuca, Hidalgo, México*
[b] *Instituto Politécnico Nacional (IPN), Centro de Investigación en Ciencia Aplicada y Tecnología Avanzada-(CICATA-Querétaro), Cerro Blanco No. 141 Col. Colinas del Cimatario, C.P. 76090, Santiago de Querétaro, Querétaro, México.*

Resumen

En este trabajo se muestran los resultados de la síntesis y caracterización de tres compuestos obtenidos a partir de latas de aluminio recicladas, los cuales fueron hidróxido de aluminio ($Al(OH)_3/SiO_2$), gamma-alúmina (γ-Al_2O_3/SiO_2) y alfa-alúmina (α-Al_2O_3/SiO_2) para ser utilizados como precursores en la síntesis de recubrimientos para la fabricación de Reflectores Difusos (RD) que pueden ser utilizados para aumentar el rendimiento de los sistemas solares, reemplazando el α-Al_2O_3 comercial. Las fases y la morfología se determinaron por Difracción de Rayos X (DRX) y Microscopía Electrónica de Barrido (MEB). La reflectancia relativa (ρd), la adhesión y la dureza se midieron por espectroscopía visible, ensayo de tracción (adhesión) y dureza de lápiz, respectivamente. El recubrimiento elaborado a partir de α-Al_2O_3/SiO_2 obtuvo los mejores resultados en todas las pruebas realizadas, presentando un ρd del 87% del espectro visible, con una dureza y adhesión de 5H y 5B respectivamente, demostrando así que la alúmina sintetizada puede reemplazar a la alúmina comercial de alta pureza como precursor en la fabricación de reflectores.

Palabras Clave: Hidróxido de aluminio, γ-alúmina/SiO_2, α-alúmina/SiO_2, Reflectores difusos, Energía solar.

Abstract

In this work is shown the results of the synthesis and characterization of three compounds obtained from recycled aluminum cans, which were aluminum hydroxide ($Al(OH)_3/SiO_2$), gamma-alumina (γ-Al_2O_3/SiO_2) and alpha-alumina (α-$Al2O_3/SiO_2$) to be used as precursors in the synthesis of coatings for the manufacture of Diffuse Reflectors (DR) that can be used to increase the performance of solar systems, replacing commercial α-Al_2O_3. The phases and morphology were determined by X-Ray Diffraction (XRD) and Scanning Electron Microscopy (SEM). The relative reflectance (ρd), adhesion and hardness were measured by visible spectroscopy, pull-through test (adhesion) and pencil hardness, respectively. The coating made from α-Al_2O_3/SiO_2 obtained the best results in all the tests carried out, presenting a ρd of 87% of the visible spectrum, with hardness and adhesion of 5H and 5B respectively, thus demonstrating that the synthesized alumina can replace high-purity commercial alumina as a precursor in the manufacture of reflectors.

Keywords: Aluminum hydroxide, γ-alumina/SiO_2, α-alumina/SiO_2, Diffuse reflectors, Solar energy.

1. Introduction

There are numerous deposits of bauxite in the world, a sedimentary rock that contains a significant concentration of aluminum minerals, mostly in the form of aluminum hydroxides and oxides (Al), which is why it is considered the most important raw material for aluminum production (Komlóssy et al., 2022). These deposits are located mainly in tropical and subtropical areas, countries such as China, Guinea, Brazil, Jamaica, Suriname, Indonesia, Malaysia and Australia (Subasinghe et al., n.d.) and it usually takes 4 to 6 tons of bauxite to produce one ton of aluminum, which causes a lot of

*Autor para la correspondencia: demetrio_fuentes@uaeh.edu.mx (Demetrio Fuentes-Hernández)
Correo electrónico: ro422009@uaeh.edu.mx (Grecia Valeria Rodríguez-Martínez), miguel_ortega@uaeh.edu.mx (Miguel Ángel Ortega-González), profe_974@uaeh.edu.mx (Felipe Legorreta-García), luis_trujillo@uaeh.edu.mx (Luis Eduardo Trujillo-Villanueva), ra422050@uaeh.edu.mx (Violeta Ramírez-Trejo), eachavezu@ipn.mx (Edgar Arturo Chávez-Urbiola)

Historial del manuscrito: recibido el 19/04/2025, última versión-revisada recibida el 05/06/2005, aceptado el 11/12/2025, en línea (postprint) desde el 07/01/2026, publicado el DD/MM/AAAA. **DOI:** https://doi.org/10.29057/icbi.v14i27.14939

deforestation during its extraction (Contreras-Bustos et al., 2003). The process begins with the extraction and refining of bauxite to obtain alumina (aluminum oxide, Al_2O_3) (Authier-Martin et al., 2001), subsequently, alumina can be obtained from the Bayer process, by electrolysis (Habashi, n.d.). Al_2O_3 occurs in various crystalline forms, highlighting gamma (γ), which has a cubic crystalline structure, and alpha (α), with a compact hexagonal structure (García Mayorga et al., 2018). Both forms exhibit exceptional physical and chemical properties. From a physical perspective, it is known for its durability, heat resistance, high hardness and reflectance to visible light, as well as its electrical insulating capacity (Le Men & Jiménez Piqué, 2009). These physical properties make it a necessary material in the manufacture of abrasives and protective coatings, among other uses (Di Prinzio & Lee, 2008).

From a chemical point of view, depending on its purity, alumina is used in applications such as the production of humidity sensors (Balde et al., 2015), enamels, paints (Roobol, 1997) and in the paper industry to improve its properties (Bajpai, 2018; Chávez Cárdenas et al., 2022).

In Mexico, although alumina is processed, there are no bauxite deposits, so it must be imported. This is because deposits are limited worldwide; consequently, one alternative for extracting aluminum is from waste containing this metal (Lee Bray, 2019). A common waste is the iconic soft drink cans, which are composed mainly of Al among other alloys, a metal that has unique properties of lightness, durability and corrosion resistance, making it essential in a variety of industrial and consumer applications (Careaga, 1993; González Martínez, 2001).

The transformation of these residues is a process that combines recycling and recovery of materials, which is why it has become an effective alternative in the search for sustainable and viable approaches in the aluminum industry (Ozer et al., 2013; Weng & Fujiwara, 2011). As environmental awareness and concerns about the depletion of natural resources grow, innovation in obtaining valuable materials from secondary sources is intensifying (Haraldson & Johansson, 2018). This approach has several significant advantages, firstly, it reduces bauxite mining, which saves resources and decreases the environmental footprint (Hong et al., 2010).

Furthermore, the processing of alumina from recycled soft drink cans contributes to the utilization of waste, offering an orderly and organized solution for managing waste before recycling. However, the need for storage facilities can also represent a logistical and economic challenge, which could be considered a negative aspect. This recycling technique helps to close the life cycle of materials, promoting the circular economy by reintroducing these products into the supply chain (Gelles, 2007; Wang et al., 2007). Alumina possesses unique properties that make it valuable in the field of optics. Due to its reflective properties, alumina has been used in the manufacture of DRs, which have become essential components in various applications involving light manipulation (Gonzalez et al., 2024). Light manipulation in this context refers to how alumina reflectors control the direction, intensity, and distribution of light to improve efficiency in solar applications. Their ability to soften and diffuse light makes these reflectors versatile tools for creating bright environments and optimizing solar energy capture, among other applications (García-Mayorga et al., 2017; Gonzalez et al., 2024). This increase in incident radiation translates into an increase of up to 80% in electrical energy production and 20 to 25% in photothermal performance, thus contributing to better performance and greater profitability of solar systems by more efficiently exploiting the available solar energy (Asvad et al., 2023; Fuentes-Hernández et al., 2020; Mohsenzadeh & Hosseini, 2015; Rönnelid Mats et al., 1999; Saitoh et al., 2003).

This technology was proposed by Tabor in 1966 (Tabor, 1966) and since then various investigations have been developed, ranging from polished metal surfaces to multilayer coatings of metals, ceramics and polymers, with ceramics showing greater resistance in environmental conditions of humidity and erosion.

(Kennedy et al., 1997) they developed low-cost, highly durable reflectors for thermal systems with reflectance exceeding 90% for at least 10 years using a layered composition of Polyethylene Terephthalate (PET), copper, silver, and alumina using Ion Beam Assisted Deposition (IBAD). The reflectors were shown to maintain their optical properties for 21 months under real-world conditions in Colorado, USA. However, they encountered manufacturing problems because the alumina deposits too slowly using this technique. This pioneering study laid the groundwork for modern polymer reflectors. Today, technologies such as thin-film mirrors in Concentrated Solar Power (CSP) plants inherit these principles, albeit with improvements in deposition and materials.

(Abd-Elhady, 2020) evaluated the impact of metallic reflectors on parabolic trough solar collectors for water desalination by analyzing the reflectivity of different materials, roughness, and desalinated water production for application in countries in the Middle East and North Africa. In their study, they determined that materials such as galvanized steel, stainless steel, and copper behave as good reflectors, reaching reflectivity values of 52, 34, and 19%, respectively. Nevertheless, they have values far from aluminum, which presented between 70 and 93%, and barium sulfate, 100%; however, the latter failed to adhere to a metallic substrate. In the specific case of aluminum, it was determined that the greater its roughness, the greater its reflective capacity.

(Gonzalez et al., 2024) they developed a ceramic-based reflector deposited on a low-carbon steel substrate with the capacity to reflect 86.95% of the visible wavelengths with high hardness (4H) and adhesion (5B) after testing different materials with high reflectance such as α-alumina (93.71%), titanium dioxide (98%) and celestite (79.81%), the first being the one that presented the best hardness and adhesion properties, providing the aforementioned values as a coating. This is of great relevance since, unlike the scarcity of mineral resources for aluminum production, Mexico's average solar radiation is 9.58 to 10.51 kWh/m^2, making it an attractive country for harnessing solar energy, whether photovoltaic or photothermal, for domestic, commercial, and industrial applications (Hernández et al., 2024). Nonetheless, this technology can not only be used in countries close to the Equator where irradiance conditions (G) are high, but on the contrary, in regions where incident solar radiation is considerably lower or where the hours of sunshine are lower, this technology can increase the generation of photovoltaic

energy or increase the operating temperature of working fluids (Rönnelid Mats et al., 1999).

(Brogren et al., 2004) They evaluated the optical properties, durability, and performance of an aluminum and PET coated steel reflector using reflectance measurement, an accelerated conditions chamber, and performance measurement in photovoltaic and photothermal systems. This resulted in a lightweight and flexible device capable of reflecting up to 82% of solar radiation under conditions in Älvkarleby, Sweden.

(Gelegenis et al., 2015) They evaluated the technical and economic feasibility of using reflectors in photovoltaic systems to increase incident solar radiation under ambient conditions in Greece, Sweden, and Japan. They found that irradiance can be increased by 10 to 30% depending on the configuration and geographic location. Specifically, a 24% increase was achieved in Sweden with reflectors 2 to 5 times the width of the panel. In Japan, a concentration 1.5 times that of normal midday conditions was achieved, and 2.7 times that of normal midday conditions if the reflectors were 2.7 times the width of the panel.

Within the framework of this research, three types of compounds were obtained, Al $(OH)_3/SiO_2$, γ-Al_2O_3/SiO_2 and α-Al_2O_3/SiO_2. These materials were obtained from aluminum cans and are intended to serve as a precursor in the synthesis of the reflective coating that was deposited on a low-carbon 1008 stainless steel substrate, such as the one developed by (Gonzalez et al., 2024), the last of these being the one that presented better reflectance.

This method of obtaining alumina is significant for reducing the environmental impact associated with electricity and water consumption in aluminum production, thus efficiently utilizing a waste product and turning it into an essential component in the manufacturing of devices that seek to enhance innovative energy processes with low environmental impact.

2. Materials and methods

The general description of the procedure used for the synthesis of the products is presented in Figure 1. Following this, the process and characterization techniques used during this research are described in detail.

2.1. Synthesis of powder compounds

2.1.1. Dissolution of Al waste

The $Al(OH)_3/SiO_2$ was obtained following the methodology of (Ibarra-Cruz et al., 2024), using aluminum cans as the raw material, with the only difference that for this study the sieving was carried out at 149 micrometers (mesh #30). In this process the can bodies were cut, milled, and sieved to obtain small particles (~ 1 mm). Subsequently, an alkaline digestion was performed with 2.5 M NaOH, with stirring (200 rpm) for 24 h at room temperature.

The products were filtered, and the resulting solution was neutralized with concentrated HCl to pH 7, yielding a white, gelatinous aluminum hydroxide. The precipitate was washed with distilled water and dried at 90 °C for 24 h.

2.1.2. Calcination of $Al(OH)_3/SiO_2$

Once the $Al(OH)_3/SiO_2$ sample was dry, it was crushed with an agate mortar and sieved to a #325 mesh to obtain fine particles, which were placed in two different crucibles to be subjected to 900 and 1400 °C to obtain γ and α alumina respectively. The heating ramp was set at 10°C/min until reaching 100°C, where it remained for 30 minutes to continue heating at the same speed, reaching the desired temperature where it was maintained for 3 h for γ-Al_2O_3/SiO_2 alumina and 6 h for α-Al_2O_3/SiO_2 alumina, depending on each sample.

2.2. Characterization of powder compounds

2.2.1. X-Ray Diffraction

The three compounds obtained together with the metallic aluminum were characterized at room temperature to identify the crystalline phases, with an INEL brand diffractometer, Equinox 2000 model, the irradiation source was CoKα1 (λ=1.789010 Å), with a curved detector, applying a voltage of 30 kV, the X-Ray diffraction patterns were indexed with the software, Crystal Impact Match.

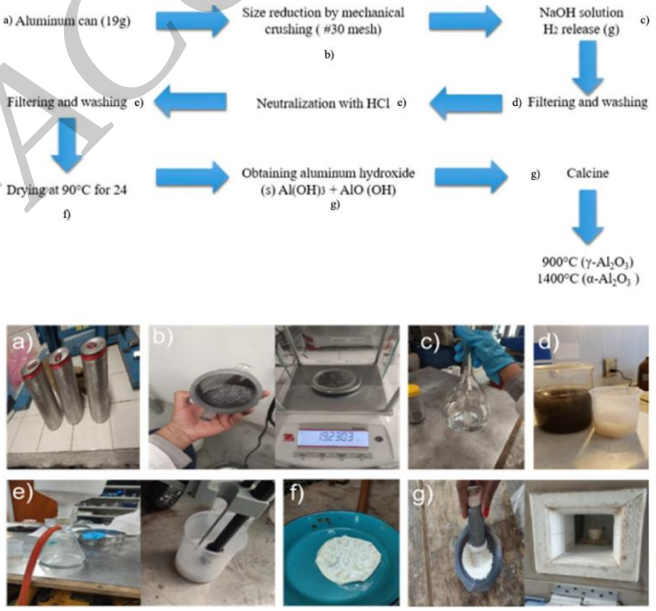

Figure 1 . Process for obtaining alumina (γ – Al_2O_3) and alumina (α - Al_2O_3).
Note: The image has been created and edited by the authors.

2.2.2. Scanning Electron Microscopy and Energy Dispersive Spectroscopy

Powder samples of the three compounds were studied using a Jeol IT 300 variable pressure scanning electron microscope. Semi-quantitative spot analyses were performed on scan areas of approximately 4.5 mm^2.

2.2.3. Measurement of relative reflectance

Once the crystalline structure was determined, the most important characterization for this study was carried out by visible light spectroscopy (VIS) using an Ocean Optics USB3000 spectrometer, calibrated with barium sulfate

provided by the manufacturer, which was considered as 100% reflectance. The analysis was carried out in the range of 400 to 800 nm to know the percentage of reflectance of each of the compounds in the visible spectrum, given that most of the semiconductor materials used in the manufacture of photovoltaic cells have the capacity to absorb and convert these wavelengths into electricity.

2.2.4. Elemental chemical composition by X-Ray Fluorescence

Metallic Al, $Al(OH)_3/SiO_2$, γ-Al_2O_3/SiO_2 and α-Al_2O_3/SiO_2 powders were analyzed to identify the chemical composition of the major elements. The analysis was performed by drying the samples at 110 °C for 2 h, 0.8 g of $Al(OH)_3/SiO_2$, alumina γ-Al_2O_3/SiO_2 and α-Al_2O_3/SiO_2, were taken and mixed with 7.8 g of lithium borate ($Li_2B_4O_7$) for fusion and obtaining a pearl. Loss On Ignition (LOI) was determined by heating 1.0 g of dry ground sample at 950 ºC for 1 h and subsequently measuring the percentage of weight loss.

2.3. Synthesis of reflective coatings

Three reflective coatings were synthesized, each with one of the compounds obtained following the methodology of (Gonzalez et al., 2024). The suspension was applied on the SAE 1008 enameled low carbon steel substrate with dimensions of 7.6 cm x 2.5 cm and a caliber of 24 (0.6 mm), by spraying with a Carman® brand 400 series gravity gun, allowing it to dry for 24 hours at room temperature, and then heat treated in an oven for 1 hour at 100°C.

2.3.1. Reflective reflectance of coatings

This property was measured in the same way, with the same equipment and same conditions as the powder compounds, to determine the variation in this optical property once the precursors were mixed with other reagents that adhere it to the substrate.

2.3.2. *Hardness evaluation (ASTM D3363)*

The test was performed on the reflective coating, this procedure is based on the pencil method, which is a widely used mechanical approach to measuring surface resistance. The ASTM D3363 reference standard provides this standard for evaluating the surface hardness of these coatings, using graphite tips (See Figure 2a).

2.3.3. *Adhesion measurement (ASTM D3359)*

The measurement was carried out using the adhesive tape method, a widely adopted mechanical approach to measuring the bond strength between the coating and the steel substrate. The ASTM D3359 reference standard establishes a standard method for assessing this property, comparing the results with descriptions and illustrations according to the guidelines of the standard shown in Figure 2. b), which shows the cross-sectional area where flaking occurred for 6 parallel cuts and the adhesion range in %. This information is key to correctly interpreting the results obtained.

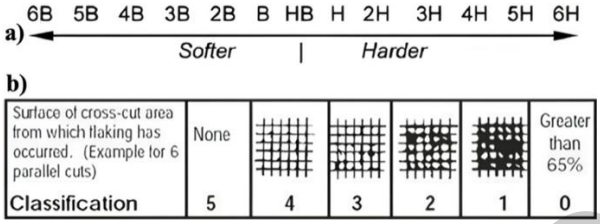

Figure 2. a) Hardness measurement and b) Adhesion measurement scale.
Note: Figures obtained from a) (Lee et al., 2020) and b) (Cai et al., 2020).

3. Results and discussion

3.1. Elemental crystallographic and chemical analysis of powdered Al and its compounds

The characteristic crystallographic planes (111), (200) and (220) were detected, with the PDF file 96-431-3211, confirming that the alloy has high contents of metallic aluminum as shown in Figure 3. The elemental composition of the Al alloy is equivalent to that reported by (Ibarra-Cruz et al., 2024), expressed in mass percentage, exhibiting a diversity of metals found, with typical values for this type of alloys according to (Davis J. R., 1993). The presence of Al in the sample is notable, representing 95.89% by mass, in agreement with the results derived from the crystallographic analysis. In addition, the presence of magnesium (Mg) and manganese (Mn) is detected at approximately 1% by mass, along with the presence of silicon (Si) and iron (Fe) at values close to 0.5% by mass. In this sense, the washing and purification process was essential to eliminate impurities formed during the synthesis due to the reaction of the rest of the elements present in the alloy and thus achieve a higher purity alumina. This can be key to achieving the desired properties in specific applications, allowing the composition to be adjusted to achieve optimal levels of reflectance, adhesion, and hardness in the final materials.

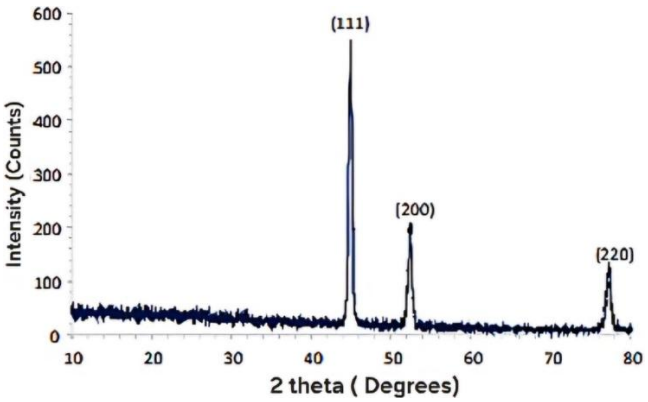

Figure 3. Diffractogram of powdered aluminum.
Note: Diffractogram generated by the authors from the experimental information.

In the case of $Al(OH)_3/SiO_2$, a loss on calcination of 21.1% was evident, while impurities of SiO_2 and NaO_2 were detected, representing 1.58% by mass. During solid-state filtration, the other components appeared as metal oxides or hydroxides. The detailed chemical composition of the sample as below, Al_2O_3 (74.400%), SiO_2 (1.58%), MgO (0.254%), CaO (0.554%), Na_2O (1.06%), Fe_2O_3 (0.027%), Cl (0.682%), P_2O_5 (0.011%), SO_3 (0.336%). The sum of these components together with the loss on ignition of 21.1% reached 100.00% total.

3.2. Crystallographic analysis of $Al(OH)_3/SiO_2$, γ-(Al_2O_3/SiO_2) and α-(Al_2O_3/SiO_2)

The $Al(OH)_3/SiO_2$ diffractogram is shown in Figure 4 (a). The identified phases correspond to the orthorhombic crystal structure of boehmite (PDF file 01-083-2384). The width and height of the peaks indicate a very small crystal size, which could suggest the presence of a high specific surface area according to (Castruita et al., 2013; Johnston et al., 2002). For b) γ-Al_2O_3/SiO_2. The identified phases correspond to the cubic crystal structure and cell parameters a = 7.9056 Å, (PDF file 01-080-0955). The width and height of the peaks indicate a small crystal size; therefore, it could also have a high surface area according to (Wen & Yen, 2000). And c) In the analysis of the α-Al_2O_3/SiO_2 powder, two distinct phases can be distinguished. The first corresponds to aluminum oxide (α-Al_2O_3/SiO_2), which exhibits a rhombohedral structure with the characteristic peaks (012) (104) (110) (113) (024) (116) and cell parameters a = 4.754 Å, c = 12.99 Å (PDF file 01-071-1683). The width and height of the peaks indicate a large crystal size according to (Jellinek & Fankuchen, 1945; Wen & Yen, 2000). On the other hand, the second phase corresponds to the aluminum and silicon oxide Al_2SiO_5, with (PDF file 01-088-0890). The presence of SiO_2 can be attributed to an impurity that could not be removed during the washing process, and which is a product of the alloying agents included in the original material.

3.3. Scanning electron microscopy of the composites SiO_2)

The micrographs of $Al(OH)_3/SiO_2$ powder are shown in Figure 5 a). Agglomerates of amorphous particles with polygonal and some circular shapes, ranging in size from 5 to 10 µm, are observed. These particles exhibit a rough surface and are composed of different sizes. Figure 5 b) shows the γ-Al_2O_3/SiO_2 alumina at x2000 magnification. Agglomerates are mostly polygonal in shape, the largest of which are between 8 and 10 µm in size, some of which have a smooth surface. Finally, in Figure 5 c) for the α-Al_2O_3/SiO_2 alumina with x2000 magnification, groups of micrometric-sized particles with more defined plate shapes can be observed, some elongated rectangular and others with polygonal shapes, most have a smooth surface and vary in size between 8 and 10 µm.

3.4. Synthesis of reflective coatings using $Al(OH)_3/SiO_2$, γ-Al_2O_3/SiO_2 and α-Al_2O_3/SiO_2

The coatings obtained are shown in Figure 6 where a) $Al(OH)_3/SiO_2$, b) γ-Al_2O_3/SiO_2 and c) α-Al_2O_3/SiO_2. It is noticeable that although the three coatings are white, they do not have the same degree of whiteness. This is due to the amount of visible radiation they are capable of reflecting; the reflectance values obtained are shown in Table 1.

3.5. Analysis of relative diffuse reflectance spectroscopy (ρd)

Table 1 shows a comparison of the results of the optical characterization of the three compounds obtained from the processing of aluminum and the coatings. In this it can be observed that the α-Al_2O_3/SiO_2 stands out for having a higher reflectance compared to the γ-Al_2O_3/SiO_2 and $Al(OH)_3/SiO_2$, this is due to its ordered crystalline structure and its uniform surface, on the contrary the $Al(OH)_3/SiO_2$ presents the lower value, this is assumed, is due to its high specific surface area as observed in Figure 5 a), which can be more porous, allowing it to reflect light diffusely. However, this porosity also translates into greater light absorption, which, in turn, is reflected in a decrease in diffuse reflectance in relation to the other compounds (Lach & Bighley, 1970; Phambu, 2003). For its part, in the case of the coatings synthesized with α-Al_2O_3/SiO_2, also it presents a higher relative reflectance compared to those obtained with the other compounds as also shown in Figure 7, this is in accordance with what was shown in the reflectance analysis of the powder compounds.

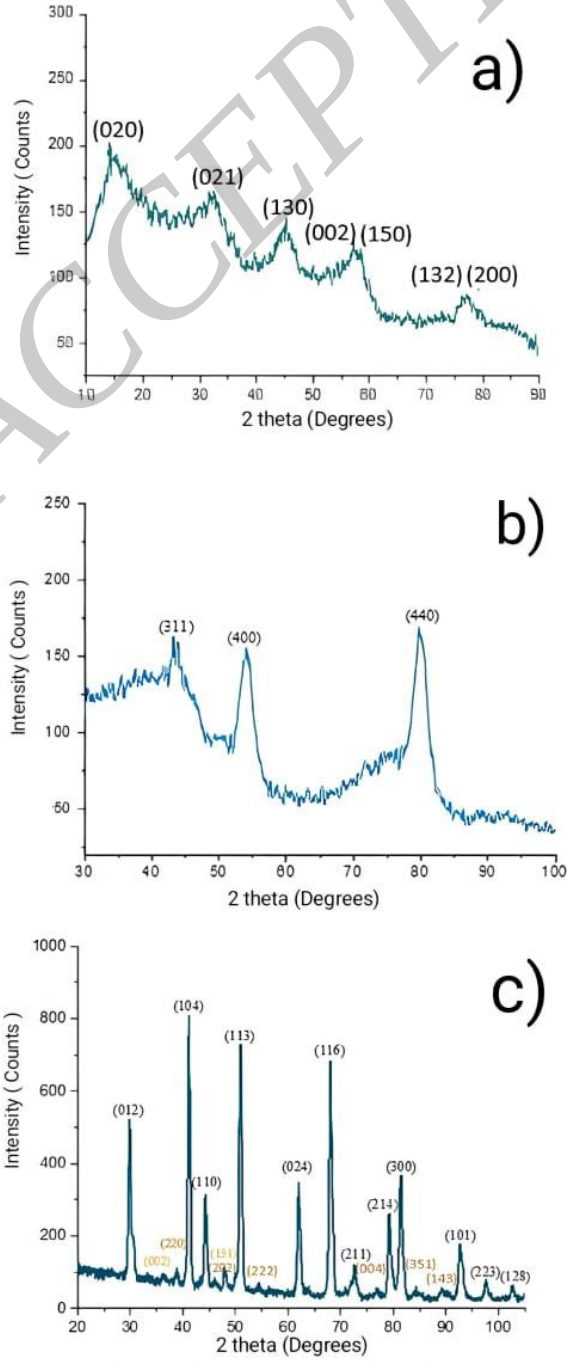

Figure 4. a) Identification of the $Al(OH)_3/SiO_2$ phases, b) γ-Al_2O_3/SiO_2 c) α-Al_2O_3/SiO_2. The orange Miller indices correspond to the aluminum and silicon oxide Al_2SiO_5.
Note: Figure created by the authors based on experimental data.

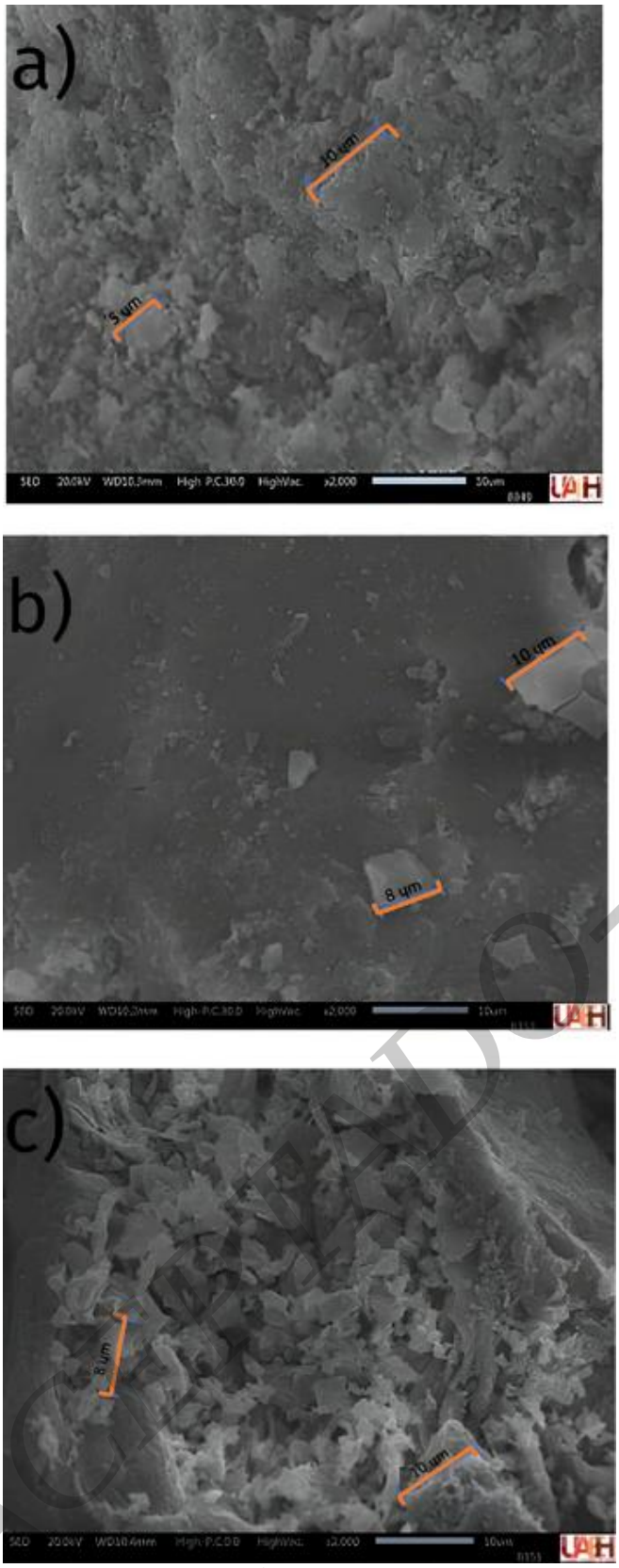

Figure 5. a) Micrograph of $Al(OH)_3/SiO_2$, b) γ-Al_2O_3 c) α-Al_2O_3.
Note: Images edited by the authors.

3.6. Hardness analysis

The same Table 1 shows the hardness results of the coatings, where the one made with $Al(OH)_3$ /SiO_2 has a value of 4H on the hardness scale. Which means that it is below γ-Al_2O_3/SiO_2 and α-Al_2O_3/SiO_2, with a value of 5H indicating that the material exhibits greater resistance to scratches and mechanical wear in the open air.

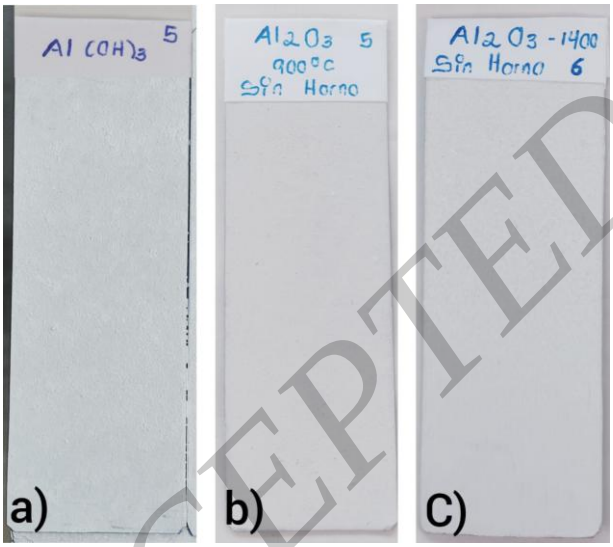

Figure 6. Coatings on the substrate of the three compounds.
Note: Images obtained by the authors of the original samples.

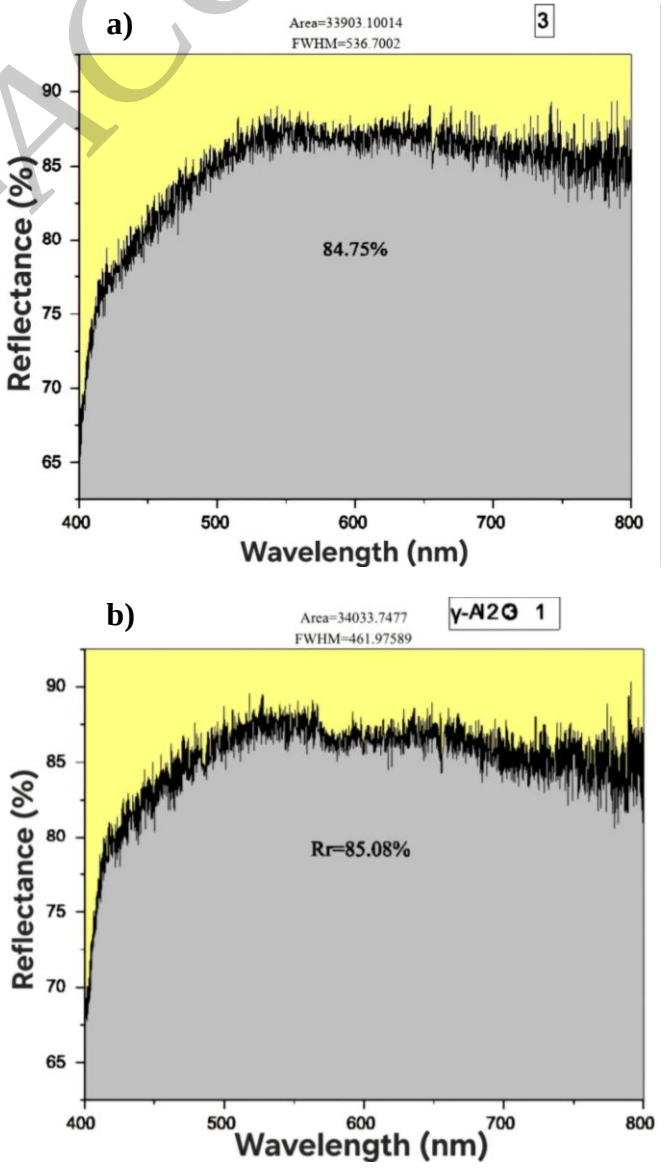

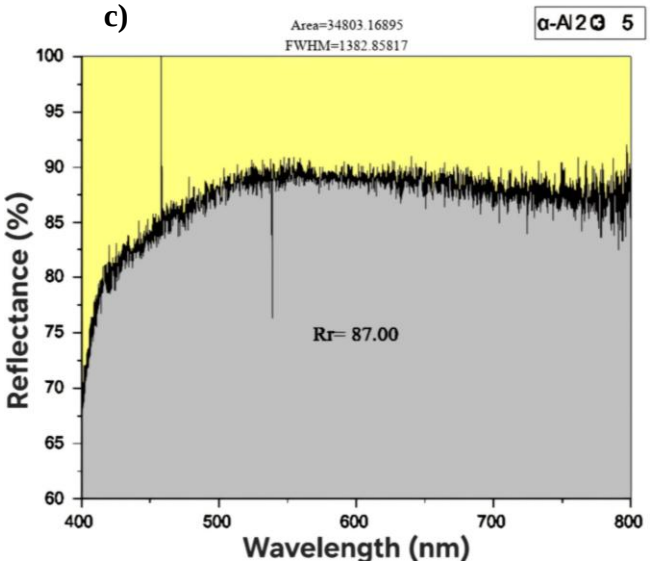

Figure 7. Reflectance spectra of a) $Al(OH)_3$ /SiO_2, b) γ-Al_2O_3/SiO_2 and c) α-Al_2O_3/SiO_2
Note: Figures obtained directly from the samples.

3.7. Adhesion analysis

In the tests of the coatings with $Al(OH)_3$)/SiO_2, γ-Al_2O_3/SiO_2 and α-Al_2O_3/SiO_2, an adhesion value of 5B was obtained for each of them, as indicated in Table 1. The excellent adhesion is attributed to the spray application, which offers significant advantages in terms of solid anchoring, layer uniformity, greater kinetic energy, favorable chemical interactions, and tensile strength.

Table 1. Relative diffuse reflectance (powders and coatings), adhesion and hardness of coatings.

Sample	ρd (%)		Adherence	Hardness
	Powder	Coatings		
$Al(OH)_3$) /SiO_2	101.37	84.75	5B	4H
γ-Al_2O_3/SiO_2	102.68	85.08	5B	5H
α-Al_2O_3/SiO_2	104.22	87.00	5B	5H
α-Al_2O_3 (Gonzalez et al., 2024)	93.71	78.31	5B	4H

4. Conclusions and discussion

Alumina from recycling may present variations in its composition due to the alloys and the production process. The latter is based on the fact that, during the analysis, other common elements were detected in aluminum alloys, which could not be eliminated in the aluminum hydroxide manufacturing process.

Scanning electron microscopy analysis of $Al(OH)_3$/SiO_2, γ-Al_2O_3/SiO_2 and α-Al_2O_3/SiO_2 powders reveals the presence of agglomerates of amorphous particles with variable shapes and sizes. While $Al(OH)_3$/SiO_2 shows polygonal and circular particles between 5 and 10 µm with a rough surface, γ-Al_2O_3/SiO_2 and α-Al_2O_3/SiO_2 present mostly polygonal agglomerates of similar size and smooth surface, although with variations in their morphology and size, this does not seem to significantly modify the reflective behavior of the material or the other mechanical properties in any of the three cases. UV-Vis spectroscopy revealed distinctive reflectance properties of the particles, highlighting the influence of porosity and crystalline structure on their optical properties. Two notable values were observed, 102.68% for γ-Al_2O_3/SiO_2 and 104.22% for α-Al_2O_3/SiO_2. In contrast, a lower diffuse reflectance was recorded for $Al(OH)_3$/SiO_2, with a value of 101.37%, which is attributed to the size of the crystalline structures and their interaction with the wavelengths of the visible spectrum. A detailed future analysis is warranted regarding the possibility of replacing α-Al_2O_3/SiO_2 with γ-Al_2O_3/SiO_2 due to the considerably lower amount of energy used in its production compared to its hexagonal counterpart and the energy that they will be able to help produce. Likewise, the hardness analysis of the coatings showed a relationship between porosity and resistance, with aluminum hydroxide showing lower resistance compared to γ-Al_2O_3/SiO_2 and α-Al_2O_3/SiO_2, however, it is noteworthy that the coatings achieved good adhesion, obtaining a uniform result of 5B on the evaluation scale, this due to the spraying method. Based on the above description and the comparison of properties in Table 1, it is concluded that α-Al_2O_3/SiO_2 can replace high-purity commercial alumina in the synthesis of coatings for the manufacture of diffuse reinforcement reflectors and, consequently, improve the generation of renewable energy from the use and recycling of aluminum waste.

Acknowledgments

We express our sincere gratitude to the members of the Ceramic Technology Laboratory (LTC, by its Spanish acronym) and to Ms. Ana Mildred Roldán Sosa for their support during the writing and review of this research work.

References

Abd-Elhady, M. S. (2020). Effect Of Metallic Reflectors And Surface Characteristics On The Productivity Rate Of Water Desalination Systems. *Thermal Science And Engineering Progress*, *17*. Https://Doi.Org/10.1016/J.Tsep.2020.100489

Asvad, M., Gorji, M., & Mahdavi, A. (2023). Performance Analysis Of A Solar Module With Different Reflectors And Cooling Flow Fields. *Applied Thermal Engineering*, *219*. Https://Doi.Org/10.1016/J.Applthermaleng.2022.119469

Authier-Martin, M., Forte, G., Ostap, S., & See, J. (2001). Overview The Mineralogy Of Bauxite For Producing Smelter-Grade Alumina. *JOM*, 36–40. Https://Doi.Org/10.1007/S11837-001-0011-1

Bajpai, P. (2018). Brief Description Of The Pulp And Papermaking Process. In *Biotechnology For Pulp And Paper Processing*. Springer, Singapore. Https://Link.Springer.Com/Chapter/10.1007/978-981-10-7853-8_2#Citeas

Balde, M., Vena, A., & Sorli, B. (2015). Fabrication Of Porous Anodic Aluminium Oxide Layers On Paper For Humidity Sensors. In *Sensors And Actuators, B: Chemical* (Vol. 220, Pp. 829–839). Elsevier B.V. Https://Doi.Org/10.1016/J.Snb.2015.05.053

Brogren, M., Helgesson, A., Karlsson, B., Nilsson, J., & Roos, A. (2004). Optical Properties, Durability, And System Aspects Of A New Aluminium-Polymer-Laminated Steel Reflector For Solar Concentrators. *Solar Energy Materials And Solar Cells*, *82*(3), 387–412. Https://Doi.Org/10.1016/J.Solmat.2004.01.029

Cai, J., Wen, Y., Wang, D., Li, R., Zhang, J., Pei, J., & Xie, J. (2020). Investigation On The Cohesion And Adhesion Behavior Of High-Viscosity Asphalt Binders By Bonding Tensile Testing Apparatus. *Construction And Building Materials*, *261*. Https://Doi.Org/10.1016/J.Conbuildmat.2020.120011

Careaga, J. A. (1993). *Manejo Y Reciclaje De Los Residuos De Envases Y Embalajes* (Vol. 4). Secretaria De Desarrollo Social (SEDESOL).

Castruita, G., Perera-Mercado, Y. A., & Saucedo-Salazar, E. M. (2013). Sol–Gel Aluminum Hydroxides And Their Thermal Transformation Studies For The Production Of A-Alumina. . *Journal Of Inorganic And Organometallic Polymers And Materials*, *23*(September 2013), 1145–1152.

Chávez Cárdenas, E. S., Chacha Palango, S., & Arias Medina, D. B. (2022). *Adición De Alúmina A Un Material Caolinítico Para Mejorar Sus Propiedades Físicas Y Químicas* [Universidad Central Del Ecuador]. Https://Www.Dspace.Uce.Edu.Ec/Server/Api/Core/Bitstreams/8d0975c2-2637-42a4-B71f-37b852a4f2dd/Content

Contreras-Bustos, R., Rosas-Cedillo, J. R., & Ruiz-García, A. J. (2003). Caracterizacion De Un Residuo Con Alto Contenido De Aluminio Characterization Of A Residue With High Aluminum Content. *Revista Mexicana De Ingeniería Química*, *2*, 109–116. Https://Rmiq.Org/Iqfvp/Pdfs/Vol.%202,%20no.%203/1.Pdf

Davis J. R. (1993). Aluminum And Aluminum Alloys. In *ASM Specially Handbook*. ASM International.

Di Prinzio, A., & Lee, Y. N. (2008). Preparación Y Caracterización De Soportes Catalíticos Esféricos De Γ-Alúmina. *Revista De La Facultad De Ingeniería U.C.V*, *23*, 47–54. Http://Saber.Ucv.Ve/Ojs/Index.Php/Rev_Fiucv/Article/View/5077

Fuentes-Hernández, D., Pérez-Vite, R., Legorreta-García, F., Vargas-Ramírez, M., & Chávez-Urbiola, E. A. (2020). Simulación Computacional Del Desempeño De Un Sistema Fotovoltaico Acoplando Generadores Termoeléctricos Y Reflectores Difusos De Refuerzo. *Pädi Boletín Científico De Ciencias Básicas E Ingenierías Del ICBI*, *8*(Especial), 128–138. Https://Doi.Org/10.29057/Icbi.V8iespecial.6335

García Mayorga, J. C., Veloz Rodríguez, M. A., & Urbano Reyes, G. (2018). *Síntesis De Alfa Alúmina Por Medio De Técnicas Electroquímicas A Partir De Chatarra De Aluminio* [Universidad Autónoma Del Estado De Hidlago]. Http://Dgsa.Uaeh.Edu.Mx:8080/Bibliotecadigital/Bitstream/Handle/231104/2368/S%C3%Adntesis%20de%20alfa%20al%C3%Bamina%20por%20medio%20de%20t%C3%A9cnicas%20electroqu%C3%Admicas%20a%20partir%20de%20chatarra.Pdf?Sequence=1&Isallowed=Y

García-Mayorga, Urbano-Reyes, G., Veloz-Rodríguez, M. A., Reyes-Cruz, V. E., Cobos-Murcia, J. A., & Hernández-Ávila, J. (2017). Preparación Electroquímica De Óxido De Aluminio (Al2o3) A Partir De Una Solución Procedente De Chatarra De Aluminio. *Tópicos De Investigación En Ciencias De La Tierra Y Materiales*, *4*(4), 179–186. Https://Repository.Uaeh.Edu.Mx/Revistas/Index.Php/Aactm/Article/View/9404/9307

Gelegenis, J., Samarakou, M., Axaopoulos, P., Misailidis, S., Giannakidis, G., & Bonaros, B. (2015). Feasibility For The Use Of Flat Booster Reflectors In Various Photovoltaic Installations. *Article In International Journal Of Renewable Energy Research*, *5*(1). Https://Www.Researchgate.Net/Publication/275637317

Gelles, G. M. (2007). Chapter 4 Aluminum Recycling Economics. In *Aluminium Recycling*.

Gonzalez, M. A. O., Urbiola, E. A. C., García, F. L., Ramírez, M. V., Hernández, D. F., Reyes, G. U., & Terven, J. (2024). Innovations In Solar Energy: Synthesis And Evaluation Of Diffuse Booster Reflector Ceramic Coating For Enhancing Thermal And Photovoltaic Systems Performance. *Energy Reports*, *12*, 2224–2231. Https://Doi.Org/10.1016/J.Egyr.2024.08.022

González Martínez, A. C. (2001). Costos Y Beneficios Ambientales Del Reciclaje En México. Una Aproximación Monetaria. *Gaceta Ecológica*, *58*, 17–26. Https://Dialnet.Unirioja.Es/Descarga/Articulo/2873746.Pdf

Habashi, F. (N.D.). A Hundred Years Of The Bayer Process For Alumina Production. In D. Donaldson & B. E. Raahauge (Eds.), *Essential Readings In Light Metals, Volume 1, Alumina And Bauxite* (First Edition, Vol. 1, Pp. 85–93). Springer International Publishing. Https://Doi.Org/Https://Doi.Org/10.1007/978-3-319-48176-0_12

Haraldson, J., & Johansson, M. T. (2018). Review Of Measures For Improved Energy Efficiency In Production-Related Processes In The Aluminium Industry – From Electrolysis To Recycling. *Renewable And Sustainable Energy Reviews*, *93*, 525–548.

Hernández, D. F., Ramírez, M. V., García, F. L., Villanueva, L. E. T., Urbiola, E. A. C., & Serrano, J. G. (2024). Computational Simulation In Solar Energy: Effect Of Passive Cooling In The Generation Of Photovoltaic Cells In Pachuca De Soto, Mexico. *Revista De Gestão Social E Ambiental*, *18*(11), E09793. Https://Doi.Org/10.24857/Rgsa.V18n11-263

Hong, J. P., Wang, J., Chen, H. Y., Sun, B. De, Li, J. J., & Chen, C. (2010). Process Of Aluminum Dross Recycling And Life Cycle Assessment For Al-Si Alloys And Brown Fused Alumina. *Transactions Of Nonferrous Metals Society Of China (English Edition)*, *20*(11), 2155–2161. Https://Doi.Org/10.1016/S1003-6326(09)60435-0

Ibarra-Cruz, L. E., Legorreta-García, F., Juárez-Tapia, J. C., Cobos-Murcia, J. Á., & Rosario-Olguin, Y. (2024). Bohemita De Tamaño Micrométrico Obtenida A Partir De Desechos Urbanos. *Pädi Boletín Científico De Ciencias Básicas E Ingenierías Del ICBI*, *11*(22), 138–143. Https://Doi.Org/10.29057/Icbi.V11i22.11026

Jellinek, M. H., & Fankuchen, I. (1945). X-Ray Diffraction Examination Of Gamma Alumina. *Industrial & Engineering Chemistry*, *37*(2), 158–163.

Johnston, C. T., Wang, S.-L., & Hem, S. L. (2002). Measuring The Surface Area Of Aluminum Hydroxide Adjuvant. *Journal Of Pharmaceutical Sciences*, *91*(7), 1702–1706.

Kennedy, C. E., Smilgys, V., Kirkpatrick, D. A., & Ross, J. S. (1997). Optical Performance And Durability Of Solar Reflectors Protected By An Alumina Coating. In *Thin Solid Films* (Vol. 304). Elsevier.

Komlóssy, G., Van Deursen, C., & Raahauge, B. E. (2022). Bauxite: Geology, Mineralogy, Resources, Reserves And Beneficiation. In Benny E. Raahauge & Fred S. Williams (Eds.), *Smelter Grade Alumina From Bauxite* (First Edition, Pp. 19–132). Springer International Publishing. Https://Doi.Org/Https://Doi.Org/10.1007/978-3-030-88586-1_2

Lach, J. L., & Bighley, L. D. (1970). Diffuse Reflectance Studies Of Solid-Solid Interactions. *Journal Of Pharmaceutical Sciences* , *59*(9), 1261–1264. Https://Doi.Org/10.1002/Jps.2600590910

Le Men, A., & Jiménez Piqué, E. (2009). *Caracterización Por Contacto De Cerámicas Nanocompuestas De Alúmina-Mullita* [Universitat Politècnica De Catalunya]. Http://Hdl.Handle.Net/2099.1/6724

Lee Bray, E. (2019). *Bauxite And Alumina*. Https://Pubs.Usgs.Gov/Myb/Vol1/2019/Myb1-2019-Bauxite-Alumina.Pdf

Lee, J. A., Lin, C. R., Pan, P. C., Liu, C. W., & Sun, A. Y. T. (2020). Dramatically Enhanced Mechanical Properties Of Diamond-Like Carbon Films On Polymer Substrate For Flexible Display Devices Via Argon Plasma Pretreatment. *Chemical Physics*, *529*. Https://Doi.Org/10.1016/J.Chemphys.2019.110551

Mohsenzadeh, M., & Hosseini, R. (2015). A Photovoltaic/Thermal System With A Combination Of A Booster Diffuse Reflector And Vacuum Tube For Generation Of Electricity And Hot Water Production. *Renewable Energy*, *78*, 245–252. Https://Doi.Org/10.1016/J.Renene.2015.01.010

Ozer, G., Yuksel, C., Comert, Z. Y., & Guler, K. A. (2013). The Effects Of Process Parameters On The Recycling Efficiency Of Used Aluminium Beverage Cans (Ubcs). *Materials Testing*, *55*(5), 396–400.

Phambu, N. (2003). Characterization Of Aluminum Hydroxide Thin Film On Metallic Aluminum Powder. *Materials Letters*, *57*(19), 2907–2913.

Rönnelid Mats, Karlsson Bjorn, Krohn Peter, & Wennerberg Johan. (1999). Booster Reflectors For PV Modules In Sweden. *Progress In Photovoltaics: Research And Applications*, *8*, 279–291. Https://Doi.Org/Https://Doi.Org/10.1002/1099-159X(200005/06)8:3<279::AID-PIP316>3.0.CO;2-%23

Roobol, N. R. (1997). *Industrial Painting Principles And Practices*. Hanser Gardner Publications.

Saitoh, H., Hamada, Y., Kubota, H., Nakamura, M., Ochifuji, K., Yokoyama, S., & Nagano, K. (2003). Field Experiments And Analyses On A Hybrid Solar Collector. *Applied Thermal Engineering*, *23*(16), 2089–2105. Https://Doi.Org/10.1016/S1359-4311(03)00166-2

Subasinghe, C. S., Ratnayake, A. S., Roser, B., Sudesh, M., Wijewardhana, D. U., Attanayake, N., & Pitawala, J. (N.D.). Global Distribution, Genesis, Exploitation, Applications, Production, And Demand Of Industrial Heavy Minerals. *Arabian Journal Of Geosciences*, 15–20.

Tabor, H. (1966). *Mirror Boosters For Solar* (Vol. 10, Issue 3).

Wang, M., Woo, K.-D., Kim, D.-K., & Ma, L. (2007). Study On De-Coating Used Beverage Cans With Thick Sulfuric Acid For Recycle. *Energy Conversion And Management*, *48*(3), 819–825.

Wen, H.-L., & Yen, F.-S. (2000). Growth Characteristics Of Boehmite-Derived Ultrafine Theta And Alpha-Alumina Particles During Phase Transformation. *Journal Of Crystal Growth*, *28*(1–4), 696–708.

Weng, Y.-C., & Fujiwara, T. (2011). Examining The Effectiveness Of Municipal Solid Waste Management Systems: An Integrated Cost–Benefit Analysis Perspective With A Financial Cost Modeling In Taiwan. *Waste Management*, *31*(6), 1393–1406.